To the Graduate Council:

I am submitting herewith a thesis written by Cara Kim Mulcahy entitled "Hydrothermal diamond anvil cell studies: a possible new calibration mineral and applications to the hydrous-carbonate mineral, nesquehonite." I have examined the final electronic copy of this thesis for form and content and recommend that it be accepted in partial fulfillment of the requirements for the degree of Masters of Science, with a major in Geology.

_____
Ted Labotka, Major Professor

We have read this thesis
and recommend its acceptance:

_____
Linda Kah

_____
Kula Misra

Accepted for the Council:

_____
Vice Chancellor and
Dean of Graduate Studies

HYDROTHERMAL DIAMOND ANVIL CELL STUDIES: A POSSIBLE NEW CALIBRATION MINERAL AND APPLICATIONS TO THE HYDROUS-CARBONATE MINERAL, NESQUEHONITE

A Thesis
Presented for the
Masters of Science Degree
The University of Tennessee, Knoxville

Cara Kim Mulcahy
December 2005

DEDICATION

This thesis is dedicated to my grandfather, Thomas W. Schoelen.

AKNOWLEDGEMENTS

I would like to thank everyone who offered their assistance to help me complete this Masters of Science degree in Earth and Planetary Sciences. In particular, I would like to thank Dr. Ted Labotka for taking in a lost soul and offering his help and guidance in the wonderful world of nesquehonite, Dr. Linda Kah and Dr. Kula Misra for all of their helpful input and for serving on my committee, Dr. Lawrence Anovitz for his patience while teaching me the quirks of the diamond anvil cell and for the synthesis of sodium niobate, Dr. Lynn Boatner and Daniel Rytz for the synthesis of barium titanate, Jonathan Evenick for his help constructing figures, and Bill Deane for his help and encouragement throughout this project.

I also like to thank Sean Mulcahy, my parents, Thomas and Trina Thompson, my brother, Kevin Thompson and my grandparents, Thomas and Bonnie Schoelen for all of their love and support.

ABSTRACT

In this study, modifications are made to the experimental setup of the Bassett-type hydrothermal diamond anvil cell facilities at the University of Tennessee. Several modifications to the HDAC setup were found to increase the number of successful experimental runs by reducing fluid loss:

- Gaskets were no longer polished or only lightly polished using 1□m diamond polishing compound. This prevented the formation of a wedge-shaped gasket.
- Gasket diameter was reduced to equal the diameter of the diamond anvil surface to prevent "tipping" of the gasket and the possible introduction of foreign material between the gasket and diamond anvils.
- Sample chamber was heated and cooled in small intervals (approximately 300 °C) rather that one large heating and cooling cycle. This reduced the amount of water loss in the sample chamber and, helped to maintain constant or nearly constant fluid pressure.

The sodium niobate structural transition most applicable to hydrothermal diamond anvil cell studies occurs at 373 °C. This transition represents a structural change from monoclinic (P) to orthorhombic (R). Unlike other transitions reported in sodium niobate, this one in particular appeared in nearly all experiments, both fluid-absent and fluid-present. The Clapeyron slope (dp/dT) of this monoclinic to orthorhombic transition appears to be negative, one of many characteristics that makes it useful as a pressure calibrant in hydrothermal diamond anvil cell experiments. Also, it was found that transitions that occurred during the heating cycle gave a better approximation of current known transition temperatures.

Currently, all thermodynamic data for nesquehonite apply to low-temperature, low-pressure conditions (<70 °C and 1 atm). Recently nesquehonite was observed as a quench phase in high-temperature, high-pressure experiments (750 °C and 50 MPa) as a result of dolomite breakdown reactions. Although nesquehonite experiments were relatively inconclusive, it is apparent from the evaluation of current thermodynamic data and tentative

experimental results from this study that the high-temperature, high-pressure stability of nesquehonite needs to be re-evaluated. Nesquehonite appears to be stable up to 205 °C at high pressure in hydrothermal diamond anvil cell experiments conducted in this study.

TABLE OF CONTENTS

LIST OF FIGURES

LIST OF TABLES

NOMENCLATURE

Abbreviations

HDAC	hydrothermal diamond anvil cell
EOS_{H2O}	equation of state of water
p	pressure
T	temperature
Atm	atmosphere
MPa	megapascal
G	Gibbs free energy
H_f	enthalpy of formation
S_f	entropy of formation
V_s	volume of solids
f_{H2O}	fugacity of water
C_p	heat capacity at constant pressure
R	gas constant (8.3144 J/mol·K)
aq	aqueous
dol	dolomite
cc	calcite
per	periclase
nesq	nesquehonite

INTRODUCTION

In this study, I investigated the application of the possible new pressure calibrant sodium niobate ($NaNbO_3$) for applicability in high-temperature, high-pressure hydrothermal diamond anvil cell (HDAC) experiments. Pressure calibration materials are useful in such studies because, currently, there is no way to measure directly sample chamber pressure during experiments. Sodium niobate is a promising candidate for use as a pressure calibrant in HDAC experiments because it has several reversible transitions, is non-reactive over a wide-range of pressure and temperature conditions, and is relatively easy to synthesize.

This study also introduces modifications developed in the Bassett-type HDAC (Bassett et al., 1993) experimental setup at the University of Tennessee, Knoxville. These findings are applied to a high-pressure, high-temperature study of the stability of the hydrous carbonate mineral, nesquehonite ($MgCO_3 \cdot 3H_2O$). To date, nesquehonite has been found almost exclusively at low-temperature, low-pressure conditions (<70 °C and 1 atm). Consequently, all published thermodynamic data apply to this pressure-temperature range. In a recent study (Labotka, personal communication), however, nesquehonite was observed as a quench phase in high-temperature, high-pressure dolomite breakdown experiments (750 °C and 50 MPa). The presence of nesquehonite in high-pressure, high-temperature conditions has important implications in carbonate diagenesis because it can act as either a source or sink for H_2O and CO_2. In this study, existing thermodynamic data for nesquehonite are evaluated for applicability at high-temperature, high-pressure conditions. The hydrothermal diamond anvil cell facilities at the University of Tennessee, Knoxville are used to determine stability of nesquehonite at these conditions.

THE HYDROTHERMAL DIAMOND ANVIL CELL (HDAC)

Introduction and Background

Traditional high-temperature, high-pressure hydrothermal experiments are conducted with some variation of a cold-seal chamber (Kerrick, 1987), piston-cylinder apparatus (Bell and Williams, 1971), or rocking autoclave (Bourcier and Barnes, 1987; Seyfried et al., 1987) constructed from precious metals such as platinum or gold or metal alloy such as silver-palladium. Although these devices provide excellent control over a wide range of temperature and pressure, the nature of the construction materials makes direct visual observation of the sample chamber during an experiment impossible. Alternative high-temperature, high-pressure cells, such as those with quartz- or sapphire-fused windows, are specifically designed for optical spectroscopic studies (Buback et al., 1987; Ohmoto et al., 1991). Unlike more traditional high-pressure hydrothermal cells, those apparatus provide direct visual observation of experiments in situ. One disadvantage is that such devices are typically limited to a small temperature and pressure range and, therefore, are not applicable to high-pressure, high temperature hydrothermal experiments. The Bassett-type hydrothermal diamond anvil cell (HDAC; Bassett et al., 1993), provides both direct visual observation of the sample chamber during experimental runs and the ability to reach a temperature of 1300°C by resistance heating (Schiferl et al., 1987; Ming et al., 1987) and a fluid pressure of up to 5.5 Mbar (Xu et al., 1986), making it ideal for many high-temperature, high-pressure hydrothermal studies.

A detailed diagram of the hydrothermal diamond anvil cell (HDAC) used in this study (Figure 1) is adapted from Furnish and Bassett (1983). The basic setup of the HDAC consists of two polished diamonds (referred to as the "upper" and "lower" diamonds) pressed on either side of a finely polished

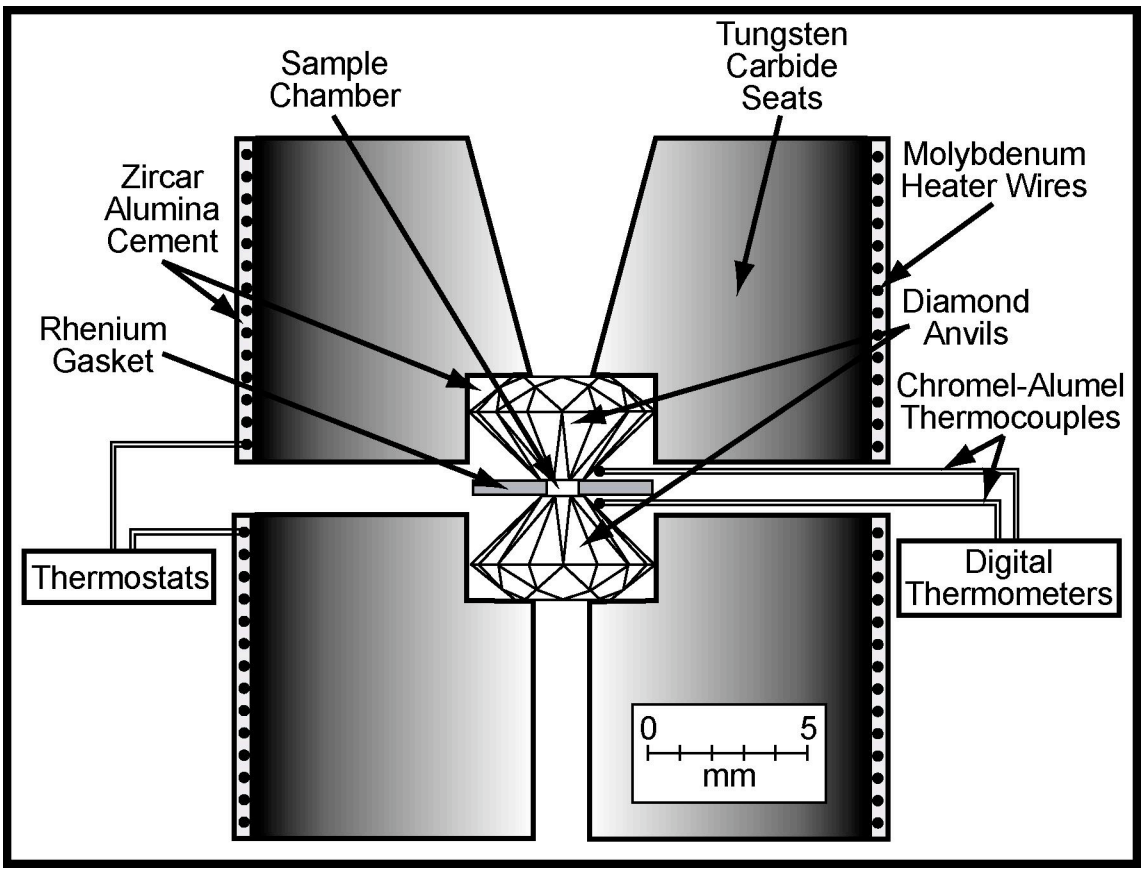

Figure 1. Bassett-type hydrothermal diamond anvil cell. The hydrothermal diamond anvil cell used in this study was adapted from Furnish and Bassett (1983).

rhenium gasket. Rhenium is used because it's hardness prevents deformation of the sample chamber during heating. The gasket has an outer diameter of 3 mm, an inner diameter of 0.5 mm, and a thickness of 125 μm, creating a sealed sample chamber with an approximate volume of 0.025 mm^3. Coiled around each diamond anvil are molybdenum heater wires and chromel-alumel thermocouples to control and measure temperature, respectively. This entire setup is held together with three screws and sealed within a stainless steel shell. A gas of 1% hydrogen and 99% argon flows around the anvil during heating to prevent oxidation of the molybdenum heater wires and diamond anvils. Pressure is created by heating a fluid medium, such as doubly de-ionized water or methanol-ethanol mixture, in a sample chamber that maintains a relatively constant volume. Experiments conducted at atmospheric pressure lack a fluid medium and, in this study are referred to as fluid absent experiments.

One difficulty in using the HDAC for hydrothermal experiments is that pressure varies during experimentation and there is no way to measure pressure directly. Various techniques are currently being used to determine pressure. Commonly, pressure calibrants such as the □-□ quartz transition (Shen *et al.*, 1993a), tetragonal to cubic transitions in $BaTiO_3$ (Chou *et al.*, 1993), $PbTiO_3$ (Chou and Haselton, 1994) and $Pb_3(PO_4)_2$ (Chou and Nord, 1994) are used to determine pressure because they have displacive structural transitions that shift with pressure-temperature conditions. Such materials are useful in HDAC studies because:

- They are relatively inexpensive and easy to synthesize
- They are non-reactive over a large region in P-T space
- They have transitions occur within a range of P-T space that is applicable to many hydrothermal studies
- Their transitions are displacive (therefore they appear rapid) and reversible
- They have transitions that are optically observable
- They have negative Clapeyron (dp/dT) slopes, resulting in phase boundaries that cross isochores of many common geologic fluids

Several pressure calibrants may be used in one experiment to improve the accuracy of the pressure determination.

Shen et al. (1992) developed another useful way to determine pressure during HDAC experiments by coupling fluid homogenization temperatures in the sample chamber with the equation of state of water (EOS_{H2O}) developed by Haar et al. (1984). Figure 2 illustrates the liquid vapor coexistence curve and density isochores calculated using NIST/ASME Steam Tables v. 2.2. Combining transition temperatures of several pressure calibrant materials with fluid homogenization temperature is the best way to improve the accuracy of pressure calculations for HDAC experiments.

Methodology

The Experimental Setup

Before each experiment, a rhenium gasket with and outer diameter of 3 mm and an inner diameter of 0.5 mm was polished using 800, 1200, 1500 and 2500 grit sandpaper and a 1 □m diamond polishing compound to eliminate gouges that may cause a fluid leak. Initially, a general parallel alignment of the diamond anvil surfaces was achieved using 99.999% silver iodide. Silver iodide is isotropic at atmospheric pressure, but when subjected to pressure, it becomes anisotropic. Alignment was achieved by squeezing silver iodide between the two diamond anvils centering the anisotropic portion by adjusting the position of each diamond. Alignment of diamond surfaces was of utmost importance

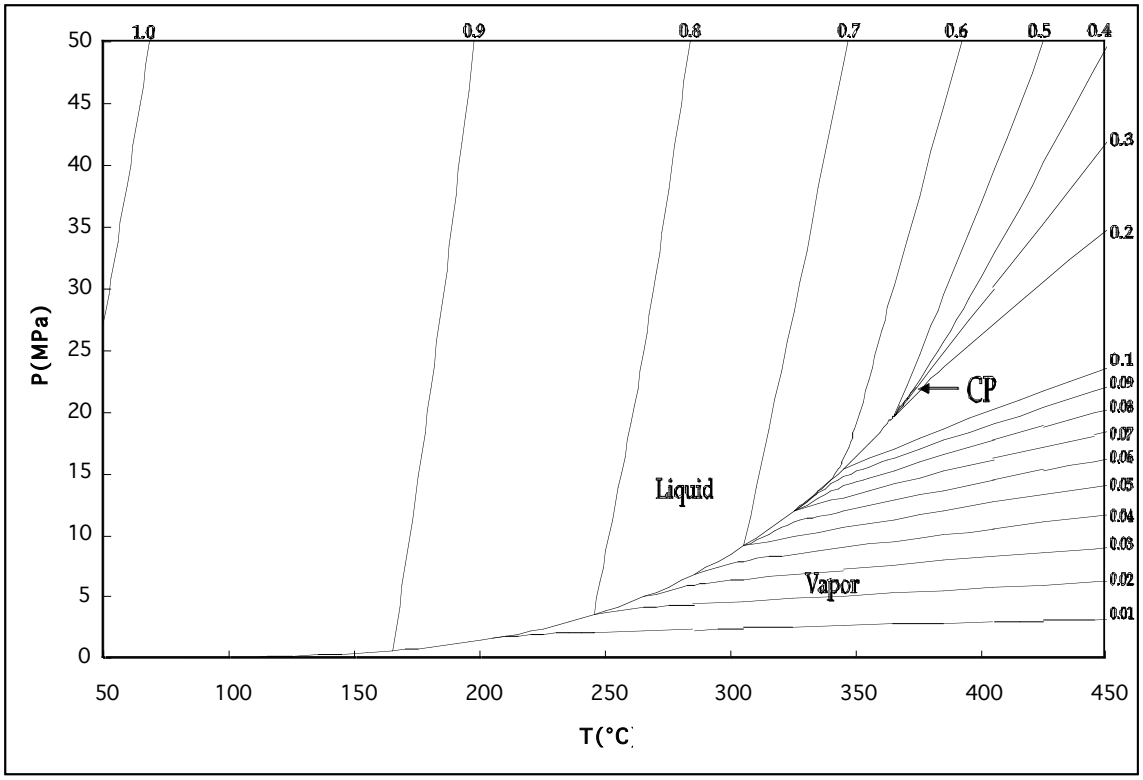

Figure 2. The liquid-vapor coexistence curve for pure water. This plot was calculated using NIST/ASME Steam Tables v. 2.2. The solid lines are density isochores in g/cm^3.

because it prevents differential stress on the diamond anvils and gaskets, which, in turn, prevents diamond shattering or fluid loss. The alignment of the diamond anvils was "fine tuned" by centering interference fringes in oil placed on the diamond anvil surfaces. After alignment, the gasket and diamond surfaces were cleaned with methanol to ensure the best possible seal. A newly polished and cleaned gasket was placed on the surface of the lower diamond (Figure 1). The sample of interest and various calibration materials (in this study, $BaTiO_3$ and $NaNbO_3$ were used) were then carefully placed into the gasket hole. When conducting a high pressure experiment, a small drop of doubly de-ionized water was suspended from the upper diamond before closing the cell (Bassett, 2003). Normally, after the fluid was loaded, a small bubble would appear in the sample chamber or a bubble was created by loosening the casing screws and retightening them the instant a small bubble formed.

The connectivity of thermocouples and heat leads was checked frequently before and after each experiment to ensure equal and efficient heating and accurate temperature readings. Connectivity was assured by placing a small drop of high-purity silver paint at each heat lead or thermocouple contact. For optimal temperature control, heat leads for upper and lower diamonds were connected to separate transformers, which, in turn, were controlled by one master transformer (Figure 3). The two smaller transformers allowed for separate control of upper and lower heat leads when temperature fluctuated vertically in the sample chamber. Upper and lower thermocouples were connected to separate temperature gauges so any temperature fluctuation could be observed. Each experiment was observed in both plane-polarized and cross-polarized light using a Nikon optical microscope with a mounted video camera.

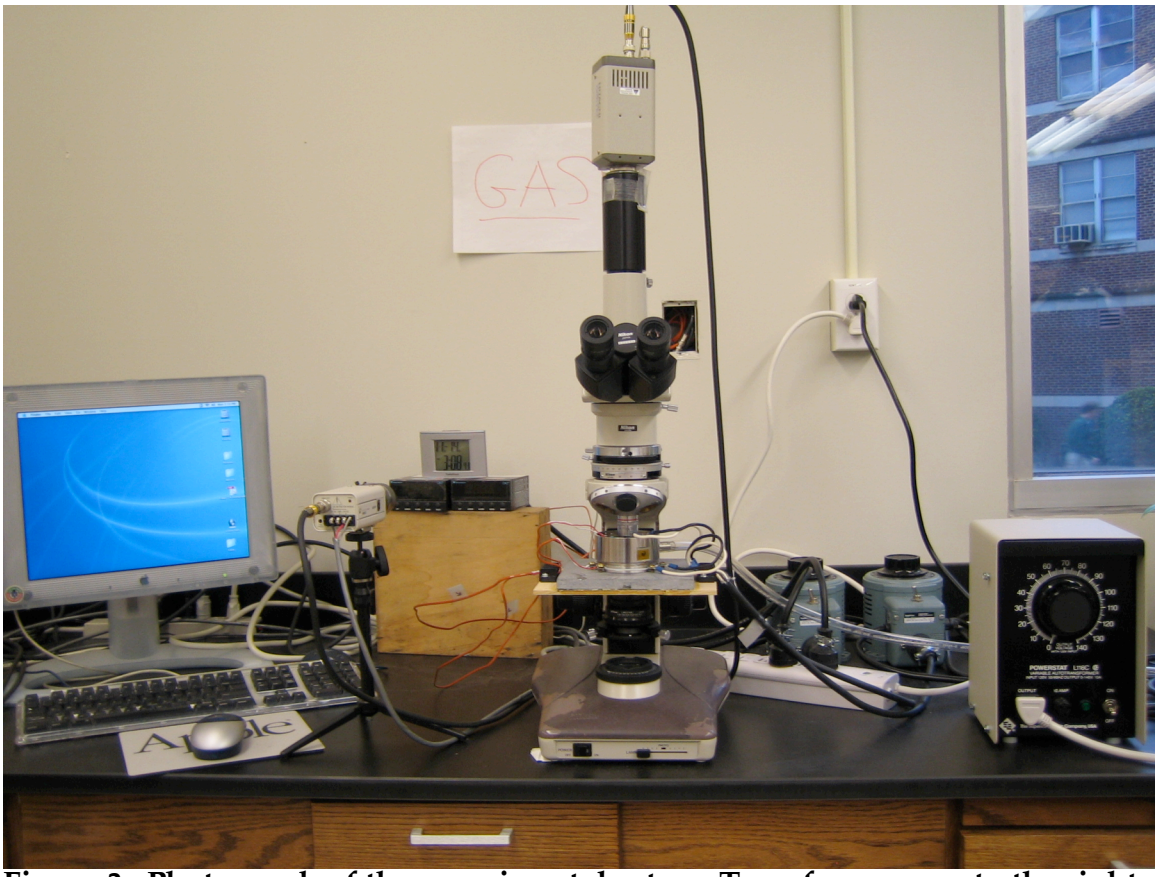

Figure 3. Photograph of the experimental setup. Transformers are to the right of the microscope. Temperature gauges are to the left.

During each experiment, video of the sample chamber, temperature readouts and a clock was recorded on computer for later study.

To determine pressure in HDAC experiments in this study, water was loaded in the cell along with a small bubble. Upon heating the bubble began to shrink; a stage in which the system is fixed to the univariant curve shown in Figure 4. At the homogenization temperature the bubble completely disappears. At this point, fluid homogenization is attained in the sample chamber, fluid density remains constant (assuming constant sample chamber volume) and the P-T relationship of the system leaves the univariant curve to follow a density isochore. At this point, the system is constrained to a single density isochore in P-T space unless, as illustrated in Figure 4, there is a change in sample chamber volume because of gasket softening during the heating cycle (Shen et al., 1992). In that case, the system travels between density isochores until the cooling cycle has begun. On the cooling cycle, Shen et al. (1992) showed that gasket size and sample chamber volume does not change significantly and, therefore, the system is constrained to one isochore. Below the homogenization temperature, the system follows the univariant liquid vapor coexistence curve. Homogenization temperatures were chosen on both the heating and cooling cycles of each experiment wherever possible. Fluid density isochores for each experiment were calculated using NIST/ASME Steam Tables v. 2.2 using fluid homogenization temperature.

Materials

The barium titanate used in this study was synthesized by the high-temperature top-seeded solution growth method by Daniel Rytz at Oak Ridge National Laboratory (Raevskii et al., 2003). Crystallinity was verified using the XRD facilities at the University of Tennessee, Knoxville.

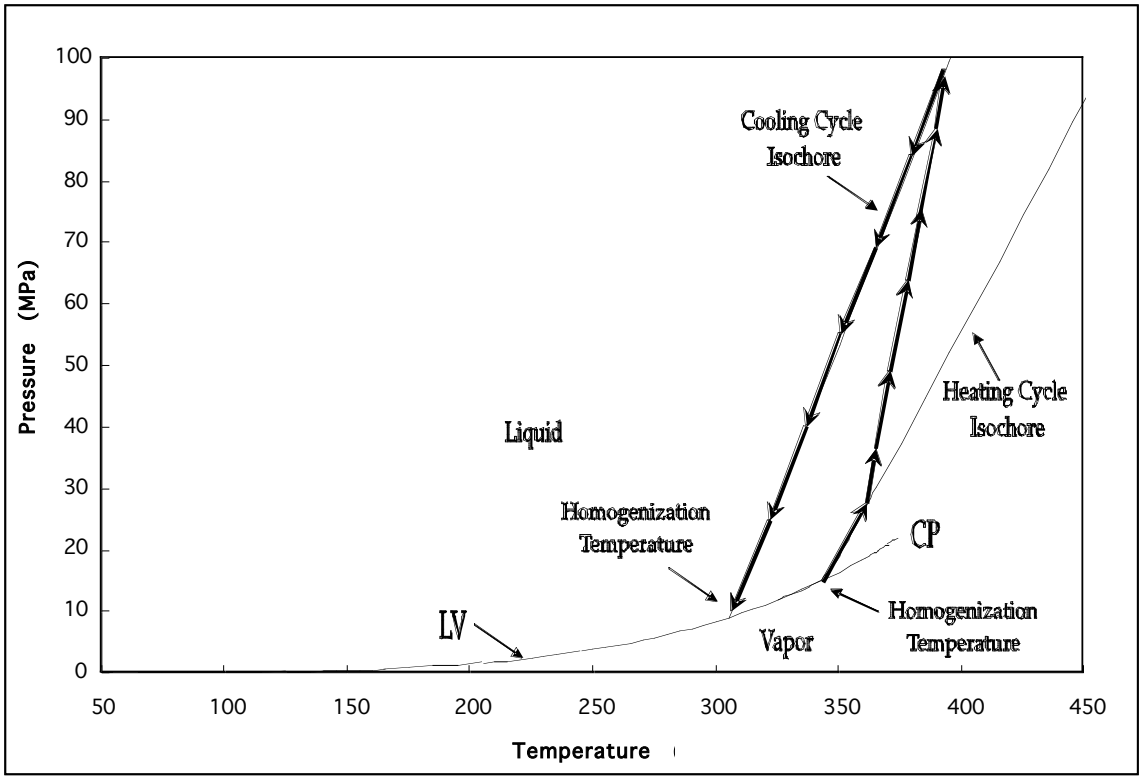

Figure 4. Pressure-temperature path of a typical HDAC experiment. This figure is adapted from Shen et al. (1992). LV is the liquid-vapor coexistence curve and CP is the critical point.

Results and Discussion

Heating and cooling the sample chamber

The sample chamber was heated and cooled at an average rate of 1 °C/s. Generally, the cell was heated from ~ 25 °C to ~ 700 °C and then cooled back down to room temperature producing one large heating and one large cooling cycle. At each observed phase transition, the temperature was either decreased or increased (depending upon current cycle) 10 to 30 °C to observe a reversal. In high-pressure, fluid-present experiments, fluid homogenization temperatures were chosen at the point when the bubble either disappeared (during the heating cycle) or reappeared (during the cooling cycle). Transition and homogenization temperatures most representative of the entire sample chamber were obtained by averaging upper and lower thermocouple readings. Both calibration materials and fluid homogenization temperatures were combined to determine pressure in the sample chamber. The tetragonal to cubic transition was identified by a change from anisotropic to isotropic in the barium titanate crystal. All transitions occurred rapidly enough to pinpoint a specific transition temperature and were easily observed in the sample chamber.

A decrease in sample chamber volume was apparent during both the heating and cooling cycles. The gasket opening shrank and deformed visibly due to softening of gasket materials. By observing changes in interference fringes, Shen et al. (1992) determined a significant decrease in the sample chamber diameter upon cell heating and, therefore a significant change in fluid density. They concluded that upon cooling, however, gasket thickness changes a maximum of 1 □m, equating to less than a 1% change in sample volume. For this reason, in fluid-rich experiments Shen et al. (1992) suggested recording transition and homogenization temperatures during the cooling cycle only. In fluid-absent experiments, this precaution is not necessary because of the absence of fluid pressure. Because of the small number of successful experiments in this study, all transition and homogenization temperatures were recorded.

Tetragonal to Cubic Transition in $BaTiO_3$ at Atmospheric Pressure

Barium titanate ($BaTiO_3$) has a perovskite-type structure. It has one displacive, tetragonal to cubic transition at approximately 120 °C and one

atmosphere (Megaw, 1947). This transition has been used for pressure determination in other HDAC studies (Bassett et al., 1996) because it occurs at temperatures applicable to many hydrothermal studies and the Clapeyron slope is negative and, therefore, intersects density isochores for water.

The barium titanate transition temperatures observed in this study ranged between 130 and 138 °C on the heating cycle and 145 and 153 °C on the cooling cycle in fluid absent experiments (1 atm). The mean transition temperatures are 132.8 °C for the heating cycle and 150.1 °C for the cooling cycle (Figure 5). The result is an approximately 8 °C range in transition temperature for any given cycle and a nearly 18 °C discrepancy between mean heating and cooling cycle transition temperatures. This variation is attributed to local strain and compositional variations in the calibration material.

Tetragonal to Cubic Transition in $BaTiO_3$ at High Pressure

Barium titanate tetragonal to cubic transition temperatures at high pressure are shown in Figure 6. Transition temperatures during the heating cycle have a negative slope and give a transition temperature of 134.5 °C at atmospheric pressure, approximately 1.7 °C off the mean transition temperature determined in fluid absent experiments (132.8 °C). Transition temperatures during the cooling cycle, however, have a positive slope and give a transition

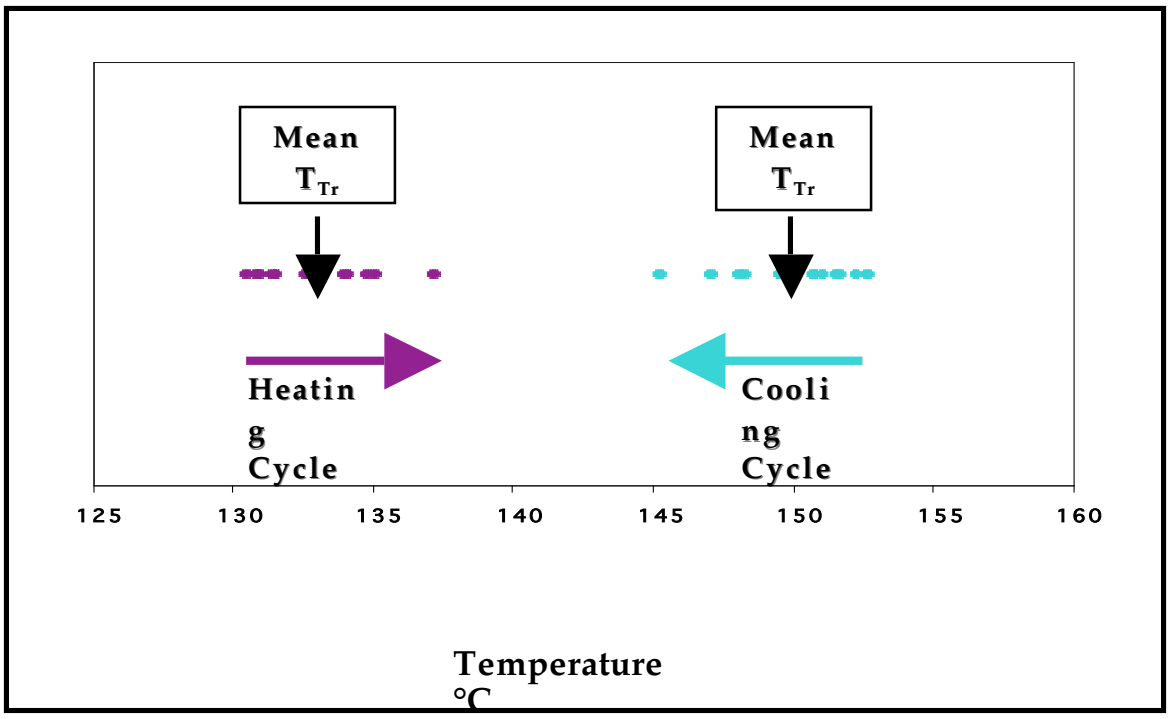

Figure 5. Tetragonal to cubic transition in $BaTiO_3$ at atmospheric pressure. Arrows represent direction of temperature change when the transition occurred.

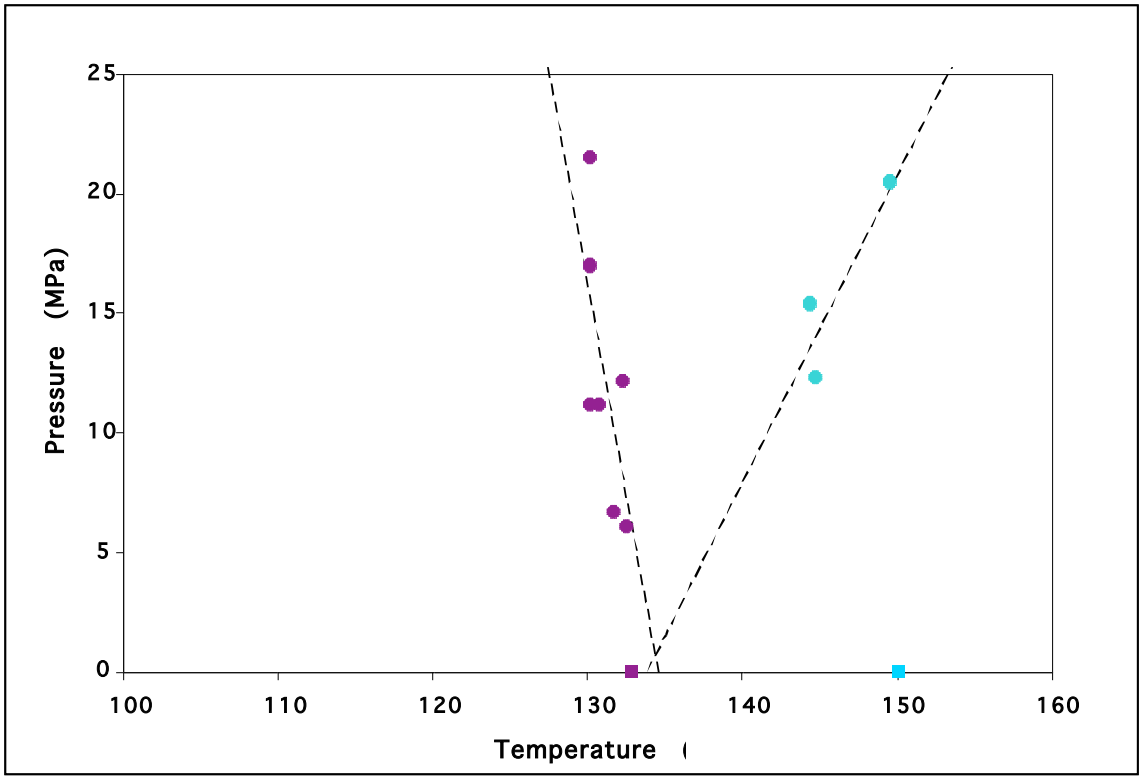

Figure 6. Tetragonal to cubic transition in $BaTiO_3$ at pressure greater than atmospheric. Purple circles represent transition temperatures on the heating cycle and blue represent the cooling cycle. Squares represent mean transition temperatures from fluid absent experiments. Dashed lines are the least squares fit for the heating and cooling cycles.

temperature of 133.8 °C at atmospheric pressure approximately 16.3 °C off the mean transition temperature determined in fluid absent experiments (150.1 °C). In contrast to the conclusion of Shen et al. (1992) that transition temperature should be taken on the cooling cycle in fluid-rich experiments, in this study transition temperatures taken on the heating cycle appear to be more accurate.

Determining Pressure

Bassett et al. (1996) developed the following equation for calculation of sample chamber pressure using the tetragonal to cubic transition in $BaTiO_3$:

$$P_{tr}\,(\text{MPa}) = 0.17 - 21.25\,[(T_{tr})_p - (T_{tr})_{LV}] \qquad (1)$$

Where T_{tr} is transition temperature, $(T_{tr})_p$ is the transition temperature at pressure of interest, and $(T_{tr})_{LV}$ is the transition temperature along the liquid vapor coexistence curve. This equation is applicable to studies using only their stock of barium titanate only because of the effect that variation in composition and local strain have on the transition temperature. Figure 7 shows the transition temperature determined by Bassett et al. (1996) and this study at varying pressure. In this study, barium titanate transitioned at approximately 134.5 °C at atmospheric pressure as opposed to ~120 °C reported by Bassett et al. (1996). For this reason, barium titanate is not used as a calibration material in this study.

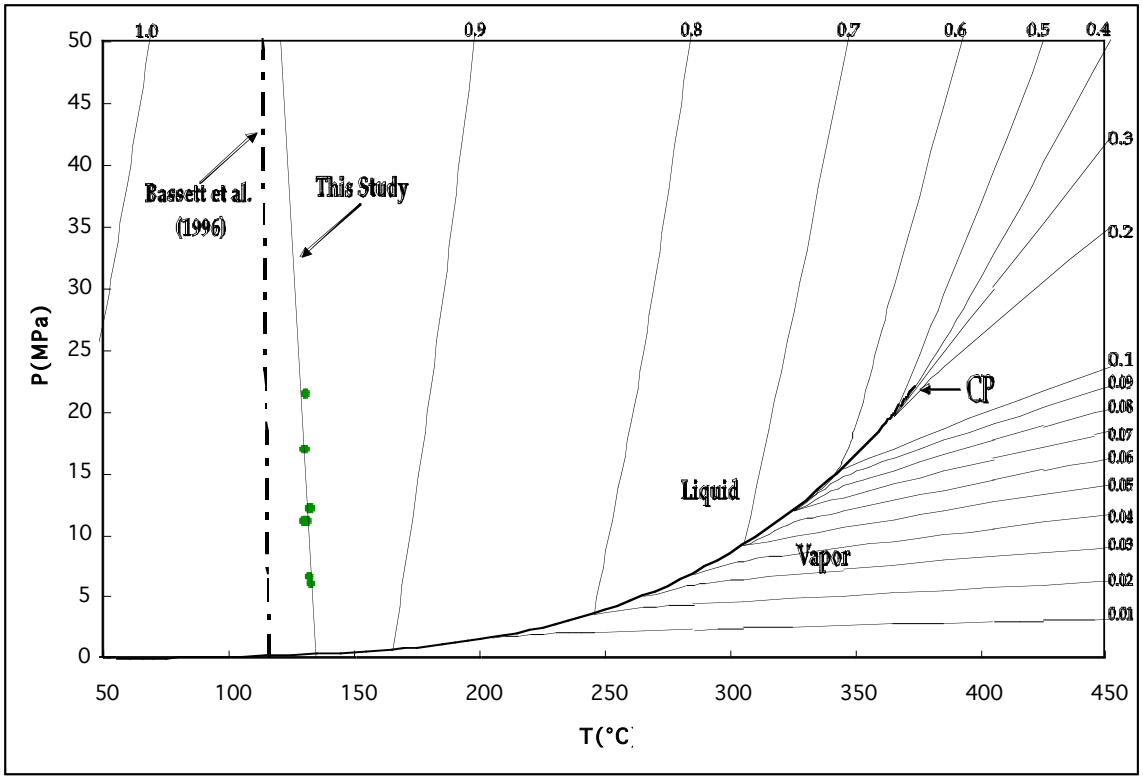

Figure 7. $BaTiO_3$ transition at high temperature and pressure in this study and as reported in the by Bassett et al. (1996). The dashed line represents transition temperatures at high pressure reported by Bassett et al. (1996). The solid line represents those found in this study.

Calibrating the Calibration Materials

As mentioned before, shifts in structural transition temperatures resulting from local variation in composition or strain in the calibration material can introduce error into the pressure determination. For this reason, calibration minerals must also undergo calibration. Shen et al. (1992, 1993b) developed a method to determine sample chamber pressure using the equation of state of water (EOS_{H2O}). They concluded that the EOS_{H2O} developed by Haar et al. (1984) provides pressures accurate to within ±1% for temperature and pressure ranges applicable to this study (< 850 °C and 1.1 GPa). The liquid vapor curve and density isochores that were calculated using NIST/ASME v. 2.2 are shown in Figure 2. Shen et al. (1992) found that the EOS_{H2O} of Haar et al. (1984) was in good agreement with pressures determined using the □-□ quartz boundary of Mirwald and Massonne (1980). For this reason, the NIST/ASME program (Haar et al., 1984) was used in my study to calculate pressure for observed fluid homogenization temperatures.

Modifications to the Experimental Setup

Several difficulties were discovered in the experimental setup. The most prominent and pervasive problem was fluid loss in the sample chamber during the cooling interval of experiments. Several techniques, including changing diamond anvil cell materials, were used in attempt to remedy this problem. First, gaskets were no longer polished prior to each experiment because it was observed that intensive polishing created a wedge-shaped gasket. Instead, either no polish or only a 1 □m diamond polishing compound was used to reduce the size of the deeper gouges in the rhenium gasket. Gasket size was also altered to prevent water loss. The outer diameter of the gasket was reduced to the same diameter of the diamond anvil surface to prevent "tipping" of the gasket that may introduce foreign material into the space between the diamond anvil surface and the gasket, thus preventing a complete seal (this, fortunately, reduced the cost of each experiment as well).

A third technique that helped prevent water loss during an experiment was heating and cooling the sample chamber in small intervals. Instead of having one heating and one cooling cycle, the sample chamber was allowed to

rest for several minutes between heating/cooling intervals of approximately 300-350 °C. Water loss was less likely to occur in such experiments. In comparison, experiments in which one cycle involved an ~650 °C of change in temperature typically lost all fluid. This phenomenon most likely results from the ability of gasket materials to soften/harden during changes in temperature. A longer "rest" time would allow gasket materials to mold to the diamond anvil surface.

Although difficulties were encountered in the experimental setup, several successful experiments were conducted that resulted in fluid homogenization as well as observed phase transitions for nesquehonite, sodium niobate, and barium titanate. These include thirteen fluid-absent experiments and nine fluid-rich experiments from which phase transition temperatures and homogenization temperatures were recorded.

HIGH-PRESSURE STRUCTURAL TRANSITIONS IN SODIUM NIOBATE

Introduction and Background

Sodium Niobate as a Possible Pressure Calibrant

One major difficulty in using the HDAC for hydrothermal studies is that the setup does not permit direct pressure measurement in the sample chamber. Currently, sample chamber pressure is determined by known phase transitions in substances such as quartz (Shen et al., 1993) and tetragonal to cubic transitions in materials such as $PbTiO_3$ (Chou and Haselton, 1994), $Pb_3(PO_4)_2$ (Chou and Nord, 1994), and $BaTiO_3$ (Chou et al., 1993). Because the pressures and temperatures at which phase transitions occur depend upon the composition of the calibration material, the equation of state of water is used to calibrate each fluid-rich experiment (Shen et al., 1992).

This study explores the applicability of shifts in phase transition temperatures in sodium niobate ($NaNbO_3$) at high-temperature, high pressure conditions for use as a pressure calibrant in hydrothermal diamond anvil cell studies. Sodium niobate is a good candidate for a possible calibration material because:

- It is relatively inexpensive and easy to synthesize
- It is non-reactive over a large region in P-T space
- It has several known phase transitions
- It has transitions that are optically observable
- These transitions occur within a range of P-T space that is applicable to many hydrothermal studies

In particular, the large number of structural transitions in sodium niobate makes it a good candidate as a possible calibration material for HDAC experiments because it would permit several possible pressure calculations from one calibrant.

Sodium Niobate Structural Transitions

At temperatures higher than 641 °C, sodium niobate has cubic perovskite structure. At temperatures lower than this, however, sodium niobate exhibits lower symmetry resulting from either a tilting of oxygen octahedra or a shift in

the position of cations (e.g. Cross and Nicholson, 1955; Ahtee and Glazer, 1974). The following six structural transitions, listed from low to high temperature, are known to occur in sodium niobate between -100 and 641 °C (Hewat, 1974);

$N(R3c) \square P(Pbma) \square R(Pmnm) \square S(Pmmn) \square T_1(Ccmm) \square T_2(P4/mbm) \square U(Pm3m)$

The temperatures at which these transitions occur at atmospheric pressure and crystal symmetries of each phase are listed in Table 1.

Yuzyuk (2005) described sodium niobate as "the most complex perovskite ferroelectric known" because of the number and the complexity of its structural transitions. Even at atmospheric pressure all phase transitions are not yet known. For instance, transitions at 150 °C and 190 °C were recently proposed on the basis of both Raman spectroscopic and dielectric studies (Wang et al., 1996; Raevskii et al., 2000). Most recent sodium niobate studies report findings on its ferroelectric properties, as it exhibits complex antiferroelectric, ferroelectric, and relaxor properties depending upon p-T conditions. Sodium niobate is paraelectric above 480 °C, antiferroelectric between 480 and -100 °C and ferroelectric below -100 °C (e.g. Shilkina et al., 1977; Henson et al., 1977).

Table 1. Structural transitions in $NaNbO_3$.

Transition Temperature	Phase	Symmetry	Reference
	N	Rhombohedral	Darlington (1971)
-100 °C	P	Monoclinic	Darlington & Knight (1999)
373 °C	R	Orthorhombic	Sakowski-Cowley et al. (1969)
480 °C	S	Orthorhombic	Ahtee, Glazer & Megaw (1972)
520 °C	T_1	Orthorhombic	Ahtee, Glazer & Megaw (1972)
575 °C	T_2	Tetragonal	Glazer & Megaw (1972)

641 °C	U	Cubic	-

Methodology

Materials

The calibration material $NaNbO_3$ was obtained from Oak Ridge National Laboratory. Sodium niobate was synthesized by Lawrence Anovitz using the methodology described by Zhelnova et al. (1983), Ivliev et al. (2003), and Raevskii et al. (2003). The crystallinity was verified using the x-ray diffractometer at the University of Tennessee (Figure 8).

Sodium niobate crystals were chosen based upon size and diaphaneity. Several crystals were chosen for each experiment to assure visibility of structural transitions through many crystal orientations. Phase transitions were identified by a change in birefringence, including the tetragonal to cubic transition at 641 °C in which the cubic phase is supposed to be isotropic. The monoclinic to orthorhombic transition was identified by a pronounced change in birefringence from high to low.

Results and Discussion

Structural Transitions

Most of the structural transitions that occurred in the sodium niobate were not always visible in experiments. For instance, the displacive tetragonal to cubic transition that occurs at 641 °C (T_2 □ U) and 1 atm was observed in few experiments. When it was observed, in both fluid-rich and fluid-absent experiments, it did not appear as a shift from anisotropic to isotropic as expected. Instead, it appeared as a dark gray to light gray shift. This discrepancy may result from compositional or structural deviations in the starting material. Other structural transitions, such as R □ S and S □ T_1 (both orthorhombic to

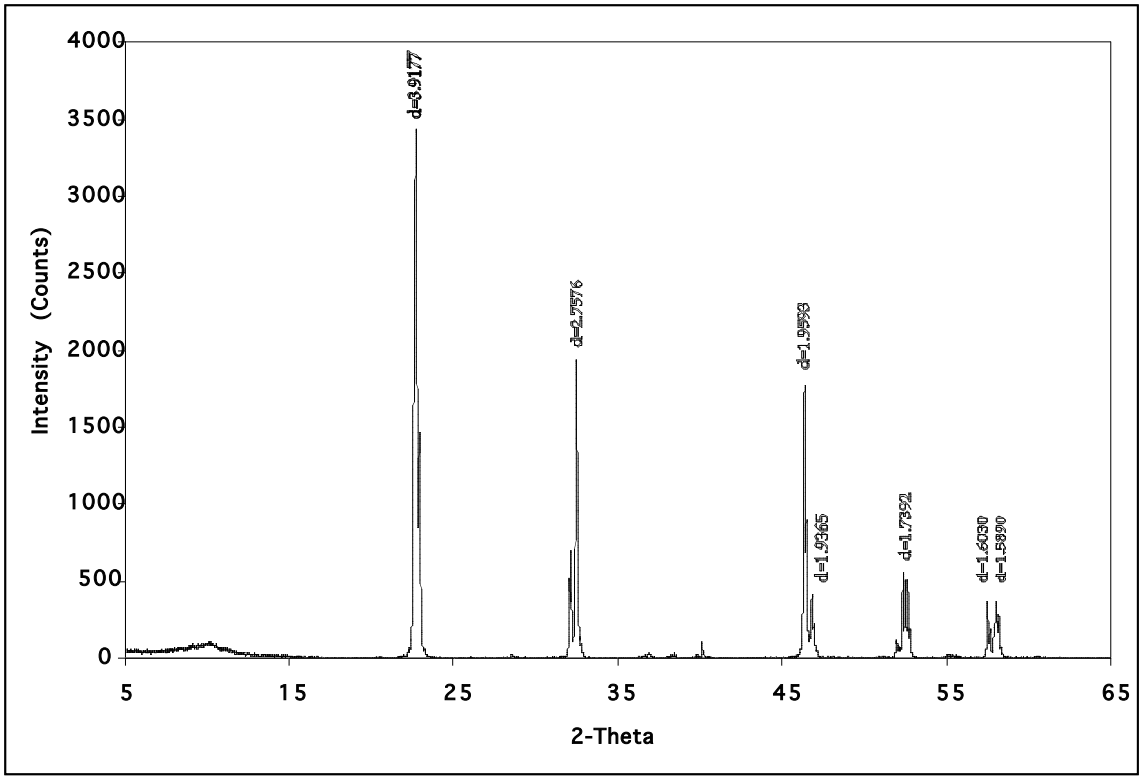

Figure 8. X-ray diffraction pattern for the room temperature (monoclinic) $NaNbO_3$ used in this study.

orthorhombic), appeared gradual (occurred over a ~ 30 °C range), making the designation of a single transition temperature difficult.

The most commonly occurring and easily observable transition is the P □ R (monoclinic to orthorhombic) transition that occurs at 373 °C. This transition was rapid enough to pinpoint a transition temperature and visible in nearly all experiments. The structure for phase P is shown in Figure 9. The structure for phase R has not yet been determined, but it is thought that the transition represents either a reorientation or disappearance of dipoles (e.g. Lefkowitz et al., 1966).

The P □ R Transition at Atmospheric Pressure

Transition temperatures for the monoclinic to orthorhombic transition agree with the transition at 373 °C reported by Sakowski-Cowley (1969). We found an average transition temperature of 372.4 °C on the heating cycle and 368.5 °C on the cooling cycle. Figure 10 shows the affect that heating or cooling rate has on the transition temperature. This figure shows that the transition temperature was reproduced best on the increasing cycle (372.4 °C). Transitions that occurred during a small decrease in temperature on the heating cycle (357.6 °C) were much lower than 373 °C and transitions that occurred during a small increase on the cooling cycle were much higher (383.2 °C). Transitions on the decreasing cycle averaged 368.5 °C. We concluded that the transition temperatures during a small increase in temperature on the heating cycle and a small decrease in temperature on the cooling cycle were closest to those reported in the literature. For this reason, in fluid-rich experiments, only transition temperatures occurring during these particular temperature cycles are reported.

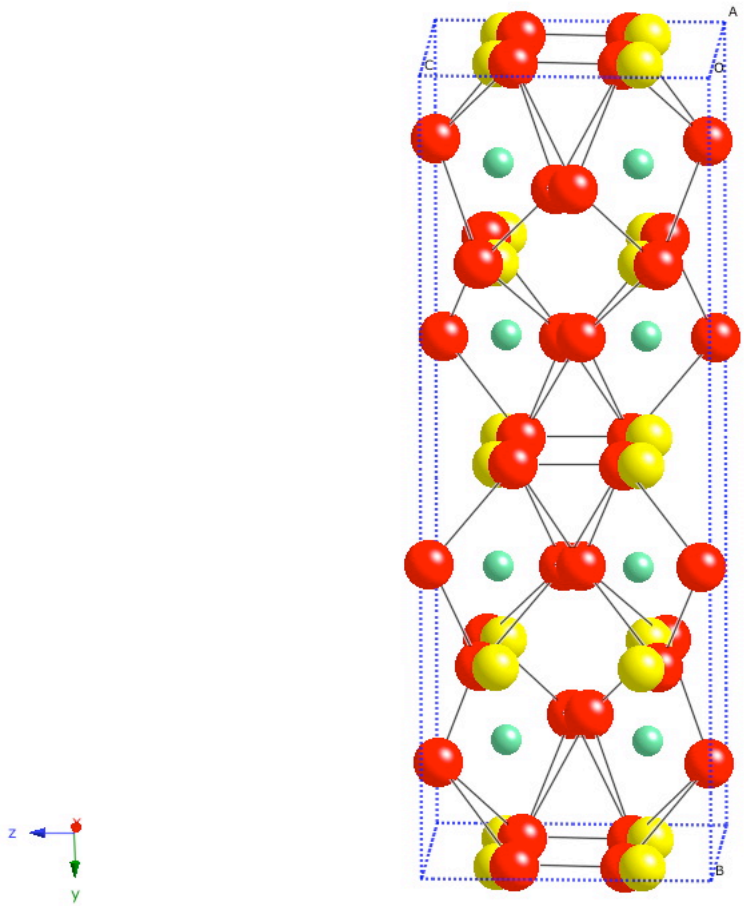

Figure 9. Structure of sodium niobate at room temperature (phase P) as reported by Sakowski-Cowley et al. (1969). Red circles are oxygen atoms, yellow are sodium and green are niobium.

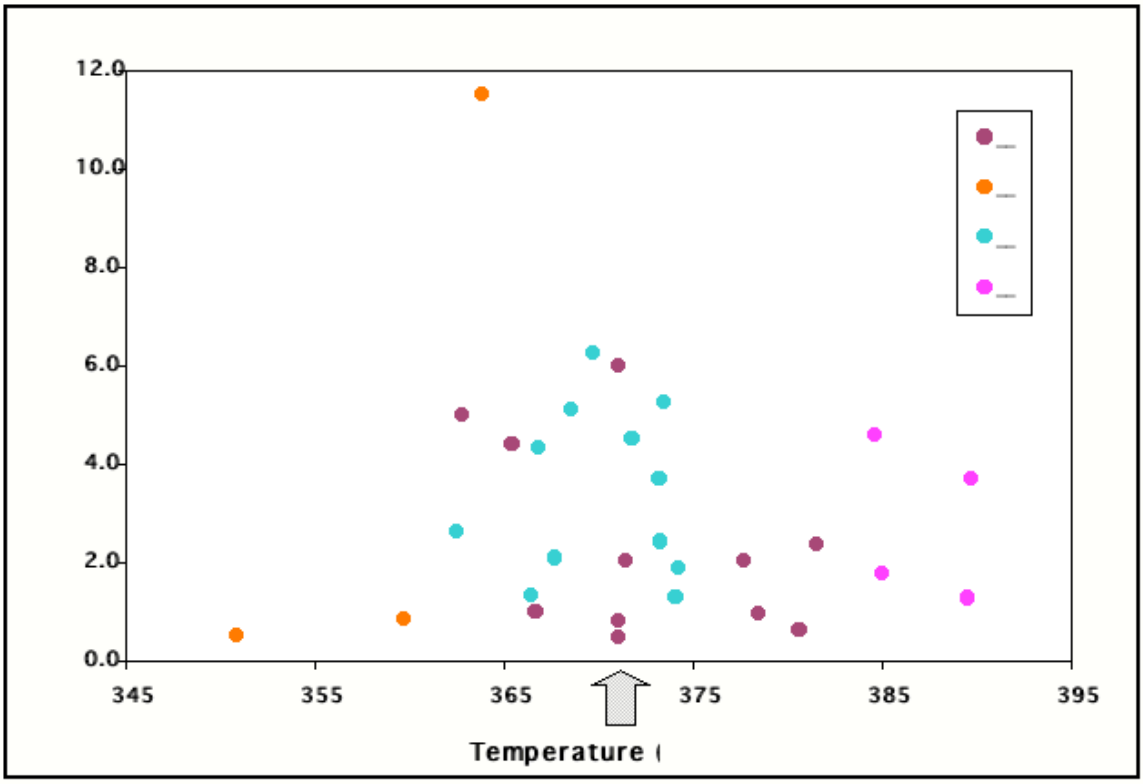

Figure 10. **P-R transition temperatures in $NaNbO_3$ at atmospheric pressure. First arrows represent heating (□) or cooling (□) cycle and second arrows represent secondary, small-scale (~30°C) heating or cooling. The large arrow represents the transition temperature at 1 atm as reported by Sakowski-Cowley et al. (1969).**

The P □ R Transition at High Pressure

The Clapeyron slope for transition temperatures is approximately -0.9 MPa/°C for the heating cycle and -0.4 MPa/°C for the cooling cycle (Figure 9). Trend lines in Figure 11 were approximated using the least squares fit. Neither the heating cycle nor the cooling cycle trends actually reproduce a temperature of 373 °C at atmospheric pressure. The slope for the heating cycle is the closest approximation for the transition temperature at 1 atm (~383.3 °C). The cooling cycle predicts a transition temperature of ~402.9 °C at 1 atm, almost 20 °C higher than the transition temperature reported by Sakowski-Cowley et al. (1969). Figure 12 shows the heating cycle data and least squares fit for the heating cycle transition temperatures in relation to the liquid vapor coexistence curve.

Application to Hydrothermal Diamond Anvil Cell Studies

The P □ R transition in sodium niobate has potential for application in high temperature, high pressure hydrothermal diamond anvil cell studies because it is rapid, reversible and occurs at temperature and pressure ranges applicable to hydrothermal studies. Other sodium niobate transitions also have potential for use in hydrothermal diamond anvil cell studies, but further study is needed.

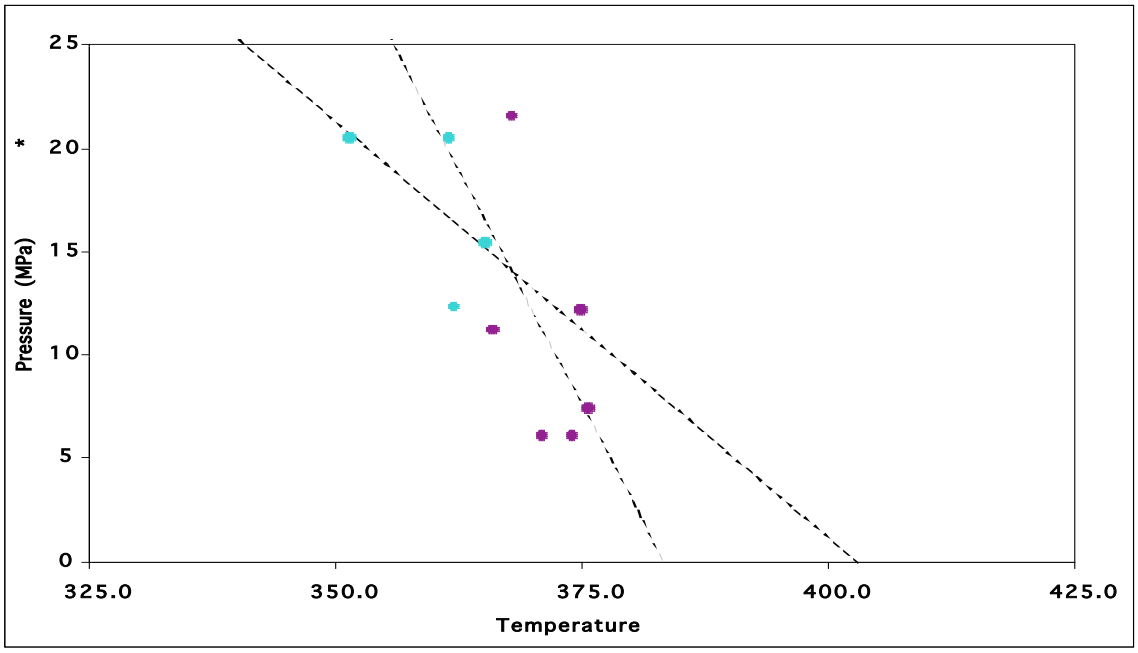

Figure 11. P-R transition temperatures in $NaNbO_3$ at pressures greater than atmospheric.

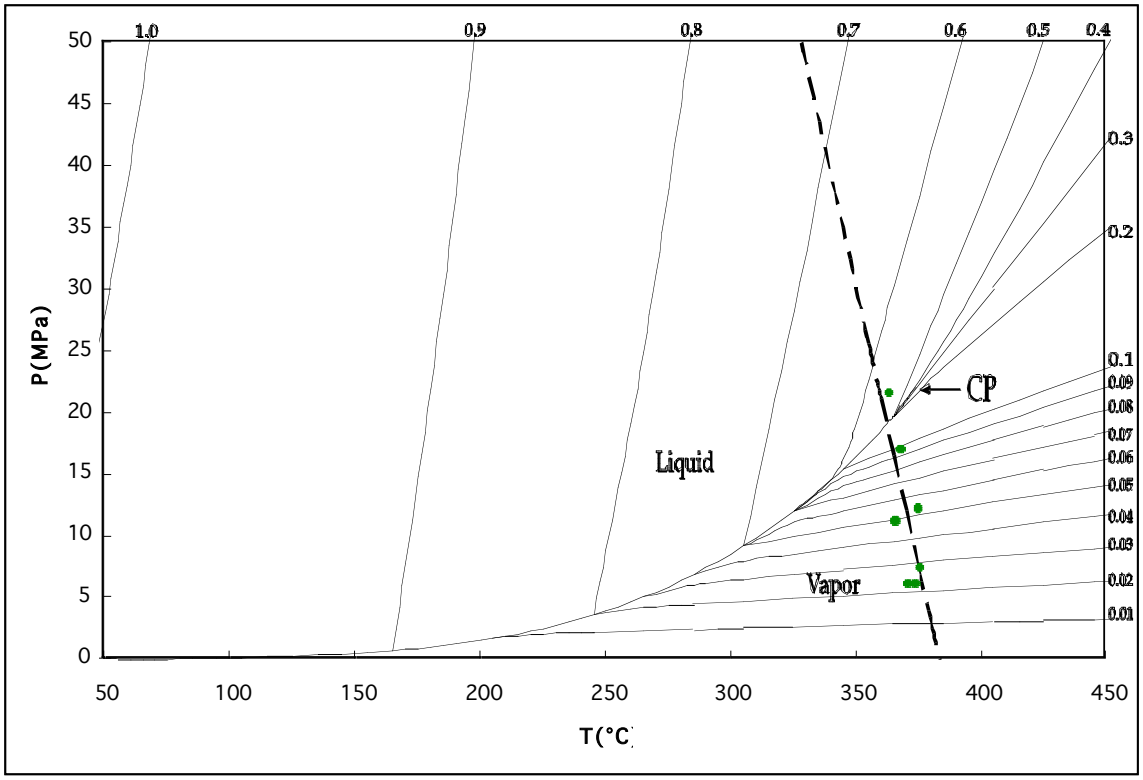

Figure 12. $NaNbO_3$ P-R transition in relation to the liquid vapor coexistence curve. The dashed line was calculated using least squares fit.

THE STABILITY OF THE HYDROUS-CARBONATE MINERAL, NESQUEHONITE

Introduction and Background

Mineral Information

Nesquehonite ($MgCO_3 \cdot 3H_2O$) is one of a suite of magnesium-carbonate minerals in the MgO-CO_2-H_2O system, including, hydromagnesite ($3MgCO_3 \cdot Mg(OH)_2 \cdot 3H_2O$), artinite ($MgCO_3 \cdot Mg(OH)_2 \cdot 3H_2O$), lansfordite ($MgCO_3 \cdot 5H_2O$), magnesite ($MgCO_3$), brucite ($Mg(OH)_2$), and periclase (MgO). It has monoclinic (pseudo-orthorhombic) symmetry, belonging to the space group $P2_1/n$ (additional crystal data listed in Table 2). Nesquehonite typically forms radiating, acicular crystals less than 4mm in length (Figure 13). It was originally found in 1888 as an accessory mineral in an anthracite coal mine in the Nesquehoning Coal Mine in Nesquehoning, Carbon County, Pennsylvania and was first reported by Genth and Penfield in 1890. Early on it was also observed at the base of stalactites (frequently referred to as "moon-milk") in association with lansfordite. Nesquehonite most commonly forms by leaching of dolomite-bearing schists and ultramafic rocks (commonly serpentine). More recently, it has been found as a weathering product on the fusion crusts of Antarctic stone meteorites (e.g. Velbel et al., 1991) and as a deposit in mineral springs and in air conditioners (Marschner, 1969). Until recently, nesquehonite is reported to be found exclusively in low-temperature, low-pressure environments.

Previous Research

A good deal of work has been done to establish the thermodynamic stability of minerals in the MgO-CO_2-H_2O system to better understand carbonate diagenesis (e.g. Langmuir, 1965; Robie and Hemmingway, 1973; Davies and

Table 2. Current thermodynamic data for nesquehonite.

	Robie & Hemingway (1972, 1973)	Helgeson (1978)
ΔG°_f	-412,035	-
ΔH°_f	-472,576	-
S°	46.76	-
V°	74.79	-
T_{tr} (°C)	340	340

$C^{\circ}p$	a	9.16E+04	2.52E+01
	b	-4.32E+02	9.13E-02
	c	5.76E-01	-4.22E+05
	d	-1.22E+09	-

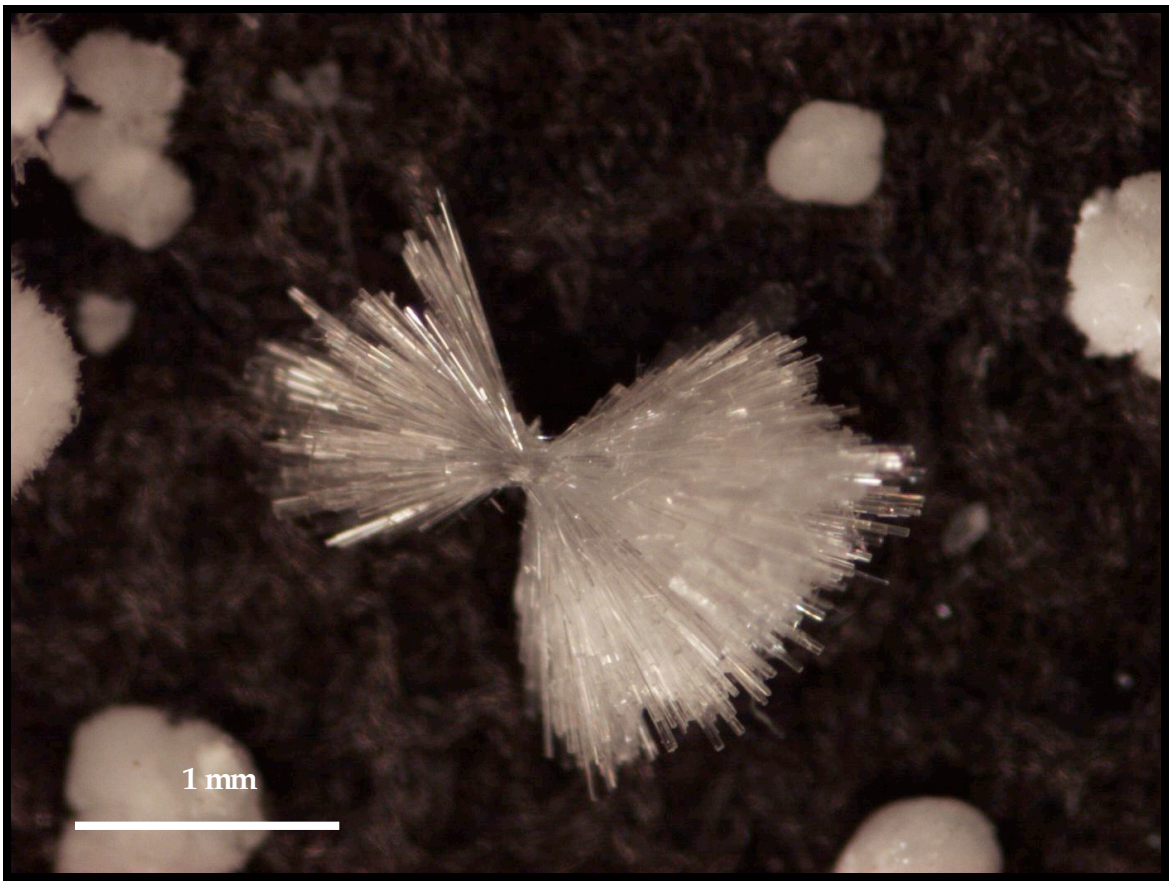

Figure 13. Cluster of nesquehonite crystals. This particular cluster came from the stock that was synthesized for this study.

Bubela, 1973). The high-temperature, high-pressure stability of nesquehonite has important implications for the thermodynamics of metamorphic rocks and conditions during carbonate diagenesis because it can act as either a source or sink for both CO_2 and H_2O. Fluid composition has major effects on the formation of carbonates. It, therefore can have a major effect on fluid composition during carbonate diagenesis.

The solubilities of minerals in the MgO-CO_2-H_2O system depend upon conditions such as pH, partial pressure of CO_2, fluid composition, temperature, and pressure. The concentration of metals such as magnesium in natural waters is dependent on the solubility of these Mg-carbonates. The dissociation of nesquehonite, in particular, has been shown to be a major control on alkalinity and can create conditions that promote the formation of dolomite (Davies et al., 1977).

Relative stabilities of nesquehonite, hydromagnesite, and lansfordite are not well established. Data reported in current literature conflict with the natural occurrence of nesquehonite and other carbonate minerals (e.g., Robie and Hemingway 1972; 1973; Davies and Bubela; 1973; Velbel, 1991; Königsberger et al., 1999). For instance, the occurrence of nesquehonite on the Antarctic stone meteorite LEW 85320 as euhedral idiomorphic crystals, rather than as pseudomorphic after lansfordite, suggests that nesquehonite forms at lower temperatures than lansfordite (Velbel et al., 1991). This disagrees with previously determined stability diagrams that suggest lansfordite forming at lower temperatures than nesquehonite (e.g. Langmuir, 1965; Ming, 1981). Velbel et al. (1991) also concluded that evaporites on meteorite fusion crusts, such as nesquehonite, consist of both terrestrial and extraterrestrial components. They suggested the need for caution when interpreting cation fractionation in these meteorites and the presence and composition of nesquehonite superposed on meteoritic fusion crusts offers important clues as to the extent of terrestrial weathering. To date, thermodynamic data reported for nesquehonite in the MgO-CO_2-H_2O system apply to low-temperature (<70 °C), low-pressure (1 atm) regions in P-T space.

High-temperature (750 °C), high-pressure (50 MPa) experimental studies have resulted in the unexpected formation of nesquehonite as a quench phase,

suggesting that the currently accepted stability range needs to be expanded (Labotka, personal communication). One experiment in particular at 750 °C and 50 MPa involved the breakdown of dolomite to form calcite and periclase:

$$CaMg(CO_3)_2 \rightarrow CaCO_3 + MgO + CO_2 \quad (1)$$

Instead of the expected reaction products, an abundance of nesquehonite was found. Labotka (personal communication) suspects that the following incongruent reaction is responsible for this mineral assemblage:

$$3H_2O + CO_{2(}aq) + MgO(aq) \rightarrow MgCO_3 \cdot 3H_2O \quad (2)$$

Reaction (2) would result in the formation of nesquehonite from the periclase produced from the dolomite breakdown reaction (1) and would account for the minor amount of periclase and the abundance of nesquehonite observed in the experiments.

Target Reaction Temperature Calculations

To determine target reaction temperatures for experiments using the hydrothermal diamond-anvil cell, stability curves for reactions in the MgO-H_2O-CO_2 system involving nesquehonite were calculated. Using Robie and Hemmingway (1972) thermodynamic values (Table 2) and the methodology presented by Langmuir (1965) and Königsberger et al. (1999), an estimate of the stability curves using the following relation was determined:

$$\Delta G\,(T,p) = \Delta H^{\circ}_f - T\Delta S^{\circ}_f + \int \Delta C^{\circ}p\,dT - T\int \Delta C^{\circ}p/T\,dT + 3RT\ln f_{H2O} + \Delta V_s(p\text{-}1) \quad (1)$$

$C^{\circ}p$ (heat capacity at constant pressure) was calculated using the following expressions (Helgeson, 1978 and Robie and Hemingway, 1972, respectively):

$$C^{\circ}p = a + bT - cT^{-2} \quad (2)$$
$$C^{\circ}p = a + bT - cT^{2} + d\sqrt{T} \quad (3)$$

Once values for C°_p were calculated, values for $\int C^{\circ}_p dT$ and $T\int C^{\circ}_p / T\, dT$ could be obtained by integration. Equation (1) gives 3 unknowns (T, p, and $\ln f_{H2O}$). To solve this expression we calculated $\ln f_{H2O}$ values at fixed temperature intervals and variable values of pressure. Calculated $\ln f_{H2O}$ values were plotted versus pressure, along with empirically determined $\ln f_{H2O}$ values from Burnham et al. (1969).

Pressure values were calculated between temperatures of 127 and 327 °C at intervals of 25 °C. Four values for pressure were determined between 152 and 227 °C. Temperature values beyond these did not result in an intersection of the two fugacity curves. These pressure and temperature values are plotted in Figure 14.

The reaction curve shown in Figure 14 is not what is expected for the dehydration reaction, nesquehonite □ magnesite + $3H_2O$. A typical dehydration reaction has a positive slope and is curved. Although no target temperatures and pressure for experimental work on the HDAC were obtained, this calculation suggests that current thermodynamic data for nesquehonite are not applicable at temperatures much greater that 67 °C and, second, that the reaction is sensitive to errors in entropy as opposed to the volume change associated with the dehydration reaction.

Methodology

Materials

Nesquehonite was synthesized at room temperature by mixing a 1.8 molar solution of K_2CO_3 and a 1.8 molar solution of $MgCl_2$. The gel that was formed upon mixing of the solutions was allowed to stand for 3 to 5 days at room temperature, covered with a watch glass. Crystals then were separated from the liquid and rinsed with deionized water and methanol to remove any residual gel. The nesquehonite was stored in a tightly sealed container at room temperature. Crystallinity was verified periodically using the XRD facilities at the University of Tennessee (Figure 15).

Experimental Results and Discussion

Experiments to determine the high-temperature, high-pressure stability of nesquehonite were inconclusive. In both fluid-rich and fluid-absent experiments, sample chamber contents were difficult to determine because of the small sample size.

Actual phase transitions were also difficult to determine in situ using only plane-polarized and cross-polarized light, and the sample was too small to determine composition using XRD analyses. Raman spectroscopy or X-ray diffraction analyses during experiments would be helpful to determine sample chamber contents.

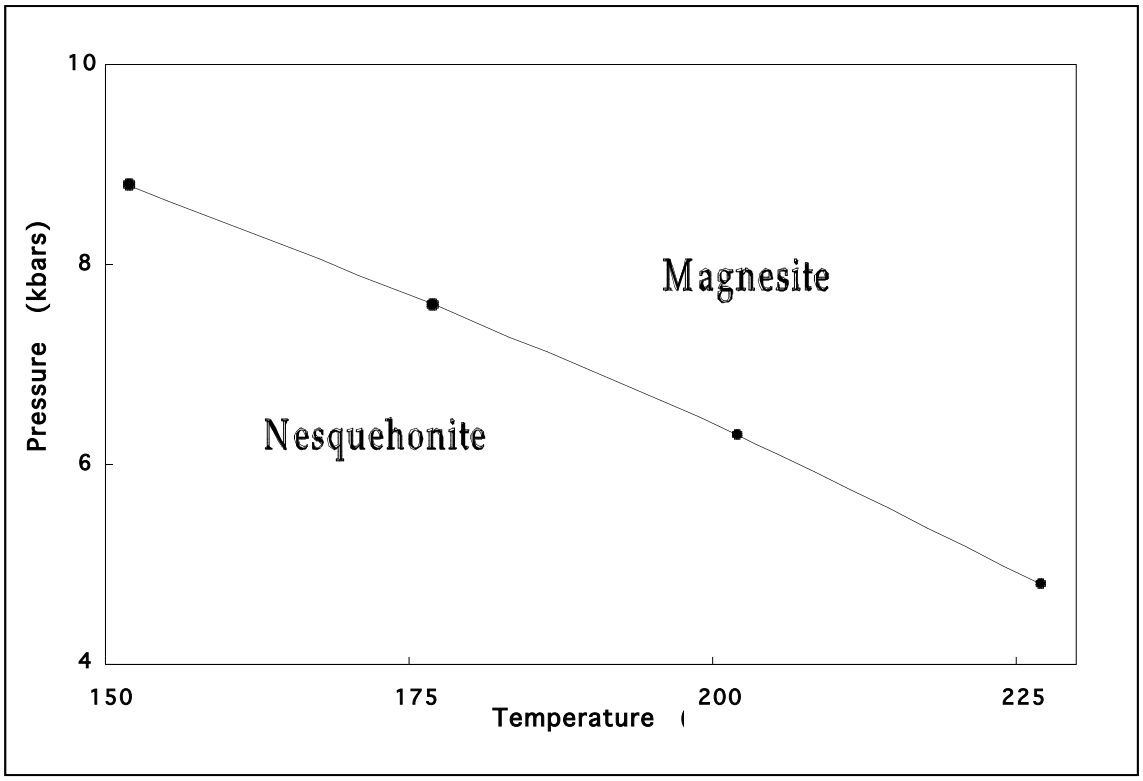

Figure 14. Calculated equilibrium curve for the dehydration reaction, nesquehonite □ magnesite + $3H_2O$.

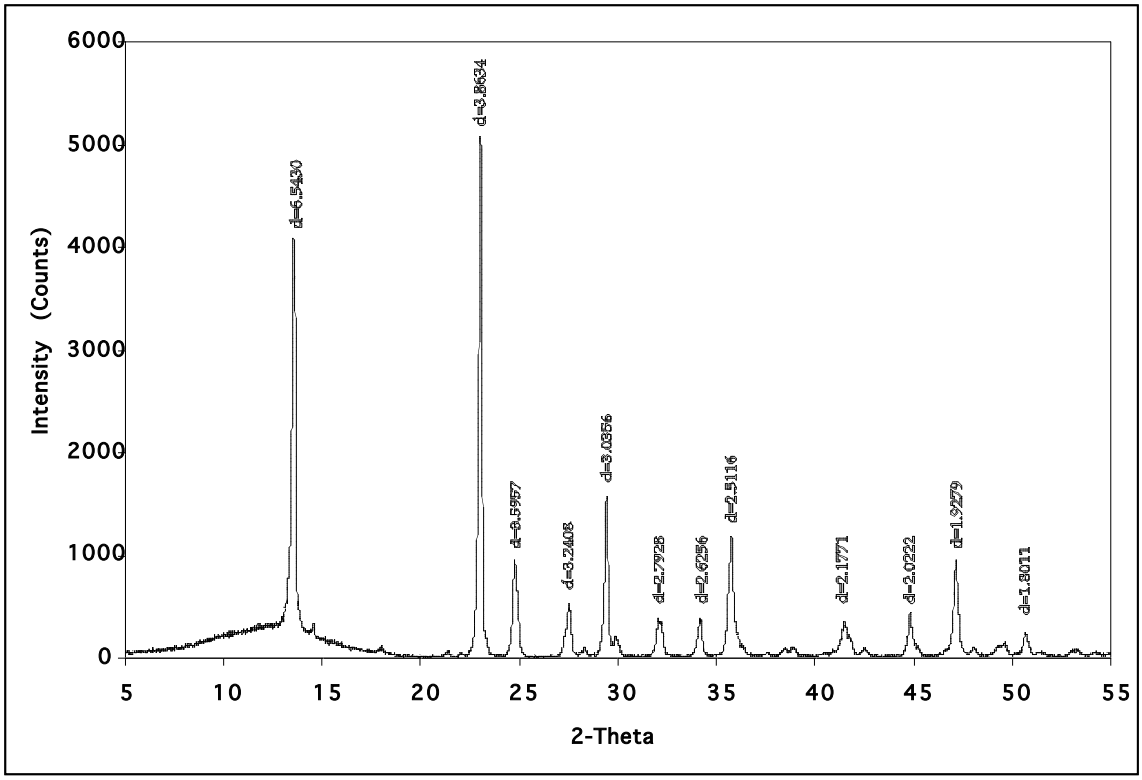

Figure 15. X-ray diffraction pattern for nesquehonite synthesized in this study.

In fluid-absent experiments, nesquehonite appeared to dehydrate at approximately 77.5 °C. This is higher than values reported in the literature (~67 °C) for the dehydration of nesquehonite. In fluid-rich experiments, the temperature of dehydration increased to between ~150 and 205 °C. Unfortunately, pressures are not known for these experiments. One experiment appeared to have resulted in complete fluid loss, in another, no bubble appeared on either the heating or cooling cycle and in the last, pressures were calculated to be atmospheric. In one experiment, nesquehonite appeared to dissolve and, upon cooling, a precipitate formed on the surface of the diamond anvils. Unfortunately, the sample was too small to perform an analysis using the XRD, but, assuming that the sample dehydrated and decarbonated, the precipitate is most likely periclase. Exactly what amount of pressure the nesquehonite crystals were actually subjected to in fluid-rich experiments is inconclusive, but they certainly appeared to be more stable at higher pressures.

DISCUSSION AND CONCLUSIONS

Several modifications were made to the Bassett-type hydrothermal diamond anvil cell experimental setup at the University of Tennessee, Knoxville, to reduce fluid loss and thereby increase the number of successful experiments. These changes include a reduction in the amount of gasket polishing, reduction in gasket diameter, and reducing heating and cooling intervals. It was also found that transitions occurring on the heating cycle better approximated current known transition temperatures for both barium titanate and sodium niobate transitions. The exact cause for this is not clear and may apply only to the HDAC experimental setup at the University of Tennessee, Knoxville.

At least one sodium niobate transition appears to be applicable to hydrothermal diamond anvil cell studies. This monoclinic (P) to orthorhombic (R) transition occurs at 373 °C and has a negative Clapeyron slope. Other observed transitions were either too gradual to pinpoint an exact transition temperature or they did not occur consistently in all experiments.

Although data for nesquehonite is inconclusive, it is apparent that its high-temperature, high pressure stability needs to be carefully re-evaluated. Current thermodynamic data for nesquehonite do not to apply to high-temperature, high-pressure conditions. In this study, nesquehonite appeared to be stable up to 205 °C and in a previous study (DeAngelis, 2005) it was observed as a quench phase in dolomite breakdown experiments that reached 750 °C and 50 MPa. More work is needed to accurately determine the high-temperature, high pressure stability of nesquehonite. HDAC studies coupled with Raman spectroscopy and/or X-ray diffraction would be useful to analyze material in the sample chamber.

REFERENCES CITED

Ahtee, M., Glazer, A.M. and Megaw, H.D. (1972) The Structures of Sodium Niobate between 480 °C and 575 °C, and Their Relevance to Soft-Phonom Modes, Philosophical Magazine, 26, 995-1014.

Ahtee, M. and Glazer, A.M. (1974) Phase transitions in sodium niobate-potassium niobate solid solutions. Ferroelectrics, 7, 93-95.

Ahtee, M. and Hewat, A.W. (1978) Structural phase transitions in sodium-potassium niobate solid solutions by neutron powder diffraction. Acta Crystallographica, Section A: Crystal Physics, Diffraction, Theoretical General Crystallography, 34, 309-317.

Bassett, W.A., Shen, A.H., Bucknum, M. and Chou, I.M. (1993) A new diamond anvil cell for hydrothermal studies to 2.5 GPa and from –190 to 1200 °C, Review of Scientific Instruments, 64, 8, 2340-2345.

Bassett, W.A., Wu, T., Chou, I., Haselton, H.T., Jr., Frantz, J., Mysen, B.O., Huang, W., Sharma, S.K. and Schiferl, D. (1996) The hydrothermal diamond anvil cell (HDAC) and its application. In: Mineral Spectroscopy: A Tribute to Roger G. Burns, The Geochemical Society, Special Publication, 5.

Bassett, W.A. (2003) High pressure-temperature aqueous systems in the hydrothermal diamond anvil cell (HDAC). European Journal of Mineralogy, 15, 773-780.

Bell, P.M. and Williams, D.W. (1971) Pressure calibration in piston-cylinder apparatus at high temperature. In Research Techniques for High Pressure and High Temperature, Eds. G.C Ulmer, Springer-Verlang, New York, 195-215.

Bourcier, W.L. and Barnes, H.L. (1987) Rocking autoclaves for hydrothermal experiments: I. Fixed volume systems. In Hydrothermal Experimental Techniques, Eds. G.C. Ulmer and H.L. Barnes, Wiley & Sons, New York, 189-215.

Buback, M., Crerar, D.A. and Koplitz, L.V. (1987) Vibrational and electronic spectroscopy of hydrothermal systems, In: Hydrothermal Experimental Techniques, Eds. G.C. Ulmer and H.L. Barnes, Wiley & Sons, New York, 333-359.

Burnham, C.W., Holloway, J.R. and Davis, N.F. (1969) Thermodynamic properties of water to 1000 °C and 10,000 bars. Geological Society of America, Special Publication, 132.

Chou, I.-M., Haselton, H.T., Jr., Nord, G.L., Jr., Shen, A.H. and Bassett, W.A. (1993) Barium titanate as a pressure calibrant in the diamond anvil cell. American Geophysical Union Transcripts, 74, 170.

Chou, I.-M. and Haselton, H.T., Jr. (1994) Lead titanate as a pressure calibrant in the diamond anvil cell. Abstract, 16th General Meeting, IMA, 74-75.

Chou, I.-M. and Nord, H.T., Jr. (1994) Lead phosphate as a pressure calibrant in the hydrothermal diamond anvil cell. GSA Abstract Program, 26, A-291.

Cross, L.E. and Nicholson, B.J. (1955) The optical and electrical properties of single crystals of sodium niobate. Philosophical Magazine, 46, 376, 453.

Darlington, C.N.W. (1971) Ph.D. Dissertation, University of Cambridge.

Darlington, C.N.W. and Knight, K.S. (1999) On the lattice parameters of sodium niobate at room temperature and above. Physica B, 266, 368-372.

Davies, P.J. and Bubela, B. (1973) The transformation of nesquehonite into hydromagnesite. Chemical Geology, 12, 289-300.

Davies, P.J., Bubela, B. and Ferguson, J. (1977) Simulation of carbonate diagenetic processes: Formation of dolomite, huntite and monohydrocalcite by the reactions between nesquehonite and brine. Chemical Geology, 19, 187-214.

Furnish, M.D. and Bassett, W.A. (1983) Investigation of the mechanism of the olivine-spinel phase transition by synchrotron radiation, 88, 10333-10341.

Genth, F.A. and Penfield, S.L. (1890) On lansfordite, nesquehonite, and a pseudomorph by nesquehonite on lansfordite. Zeitschrift für.. Krystallographie und Mineralogie, 17, 561.

Glazer, A.M. and Megaw, H.D. (1972) The Structure of Sodium Niobate (T_2) at 600 °C, and the Cubic–Tetragonal Transition in Relation to Soft-Phonon Modes, Philosophical Magazine, 25, 1119-1135.

Haar, L., Gallagher, J. and Kell, G.S. (1979) Water and Steam: Their properties and current industrial applications. In: J. Straub and K. Scheffler, Eds., Thermodynamic properties for fluid water. Proceedings 9th International Conference Properties of Steam, Pergamon Press, New York, 69-82.

Haar, L., Gallagher, J.S. and Kell, G.S. (1984) NBS/NRC Steam Tables. Thermodynamic and transport properties and computer programs for vapor and liquid states of water in SI units. Hemisphere Publishing Co., Washington D.C.

Helgeson, H.C., Delany, J.M., Nesbitt, H.W. and Bird, D.K. (1978) Summary and critique of the thermodynamic properties of rock forming minerals. American Journal of Science, 278-A.

Henson, R.M., Zeyfang, R.R. and Kiehl, K.V. (1977) Dielectric and electromechanical properties of (Li-Na)NbO_3 ceramics. Journal of American Ceramics Society, 60, 15.

Hewat, A.W. (1974) Neutron powder profile refinement of ferroelectric and antiferroelectric crystal structures: sodium niobate at 22 °C. Ferroelectrics, 52, 83.

Ivliev, M.P., Raevskii, I.P., Reznichenko, L.A., Raevskaya, S.I. and Sakhnenko, V.P. (2003) Phase states and dielectric properties of sodium-potassium niobate solid solutions. Physics of the Solid State, 45, 10, 1984-1989.

Kerrick, D.M. (1987) Cold-seal systems. In Hydrothermal Experimental Techniques, Eds. G.C. Ulmer and H.L. Barnes, Wiley & Sons, New York, 293-323.

Kinsolving, M.R., MacGillavry, C.H. and Pepinsky, R. (1950) Twinning in nesquehonite, $MgCO_3 \cdot 3H_2O$. American Mineralogy, 35, 127.

Königsberger, E., Königsberger, L. and Gamsjäger, H. (1999) Low-temperature thermodynamic model for the system Na_2CO_3 – $MgCO_3$ – $CaCO_3$ – H_2O. Geochimica et Cosmochimica Acta, 63, 19/20, 3105-3119.

Langmuir, D. (1965) Stability of carbonates in the system MgO-CO_2-H_2O. Journal of Geology, 73, 730-754.

Lefkowitz, I., Łukaszewicz, K. and Megaw, H.D. (1966) The high-temperature phases of sodium niobate and the nature of transitions in pseudosymmetric structures. Acta Crystallographica, 20, 670-683.

Marschner, H. (1969) Hydrocalcite ($CaCO_3 \cdot H_2O$) and nesquehonite ($MgCO_3 \cdot 3H_2O$) in carbonate scales. Science, 165, 1119-1121.

Megaw, H.D. (1947) Temperature changes in the crystal structure of barium titanium oxide. Proceedings of the Royal Society of London, A, 89, 261.

Megaw, H.D. (1974) The seven phases of sodium niobate, Ferroelectrics, 7, 87.

Ming, D.W. (1981) Chemical and crystalline properties of minerals in the MgO-CO_2-H_2O system. M.S. thesis, Colorado State University.

Ming, L.-C., Manghnani, M.H. and Balogh, J. (1987) Resistive heating in the diamond-anvil cell under vacuum conditions. In: High-Pressure research in Mineral Physics, Eds. M.H Manghnani and Y. Syono, Terra Science Publication Company, AGU, Tokyo, Japan/Washington D.C. 69-74.

Mirwald, P.W. and Massonne, H.-J. (1980) The low-high quartz and quartz-coesite transition to 40 kbar between 600 °C and 1600 °C and some reconnaissance data on the effect of $NaAlO_2$ component on the low quartz-coesite transition. Journal of Geophysical Research, 85, 6983-6990.

Ohmoto H., Hayashi, K., Onuma, K., Tsukamoto, K., Kitakaze, A., Nakano, Y. and Yamamoto Y. (1991) Solubility and reaction kinetics of solution-solid reactions determined by in situ observations. Nature, 351, 634-636.

Raevskii, I.P., Reznichenko, L.A., Smotrakov, V.G., Eremkin, V.V., Malitskaya, M.A., Kuznetsova, E.M. and Shilkina, L.A. (2000) A New Phase Transition in Sodium Niobate. 26, 8, 744-746.

Raevskii, I.P., Reznichenko, L.A., Ivliev, M.P., Smotrakov, V.G., Eremkin, V.V., Malitskaya, M.A., Shilkina, L.A., Shevtsova, S.I. and Borodin, A.V. (2003) Growth and study of single crystals of (Na,K)NbO_3 solid solutions. Crystallography Reports 48, 3, 486-490.

Robie, R.A. and Hemingway, B.S. (1972) The heat capacities at low-temperature and entropies at 298.15 K of nesquehonite $MgCO_3 \cdot 3H_2O$, and hydromagnesite. American Mineralogist, 57, 1768-1781.

Robie, R.A. and Hemingway, B.S. (1973) The enthalpies of formation of nesquehonite, $MgCO_3 \cdot 3H_2O$, and hydromagnesite, $5MgO \cdot 4CO_2 \cdot 5H_2O$. Journal of Research U.S. Geological Survey, Sept.-Oct., 1, 5, 543-547.

Sakowski-Cowley, A.C., Łukaszewicz, K. and Megaw, H.D. (1969) The structure of sodium niobate at room temperature, and the problem of reliability in pseudosymmetric structures. Acta Crystallographica, B25, 851-865.

Schiferl, D., Fritz, J.N., Katz, A.I., Schaefer, M., Skelton, E.F., Qadri, S.B., Ming, L.C. and Manghnani, M.H. (1987) Very high temperature diamond-anvil cell for x-ray diffraction: Application to the comparison of the gold and

tungsten high-temperature-high-pressure internal standards. In: High-Pressure Research in Mineral Physics, Eds. M.H. Manghnani and Y. Syono, Terra Science Publication Company, AGU, Tokyo, Japan/Washington D.C., 75-83.

Seyfried, W.E., Janecky, D.R. and Berndt, M.E. (1987) Rocking autoclaves for hydrothermal experiments: II. The flexible reaction-cell systems. In Hydrothermal Experimental Techniques, Eds. G.C. Ulmer and H.L. Barnes, Wiley & Sons, New York, 216-239.

Shen, A.H., Bassett, W.A. and Chou, I-Ming. (1992) Hydrothermal studies in a diamond anvil cell: Pressure determination using the equation of state of H_2O. In: High-Pressure Research: Application to Earth and Planetary Sciences, Eds. Y. Syono and M.H. Manghnani, Terra Scientific, Washington D.C., 61-68.

Shen, A.H., Bassett, W.A. and Chou, I-Ming. (1993a) The □-□ quartz transition at high temperatures and pressures in a diamond-anvil cell by laser interferometry. American Mineralogist, 78, 694-698.

Shen, A.H., Chou, I.-M. and Bassett, W.A. (1993b) Experimental determination of isochores of H_2O in a diamond-anvil cell up to 1200 MPa and 860 °C with preliminary results in the NaCl-H_2O system. In: Proceedings of the 4th International Symposium on Hydrothermal Reactions, Nancy, France, Aug.–Sept. 3, 235-239.

Shilkina, L.A., Reznitchenko, L.A., Kupriyanov, M.F. and Fesenko, E.G. (1977) Phase transitions in the $(Na_{1-x}\text{-}Li_x)NbO_3$ solid-solution system. Soviet Physics-Technical Physics, 22, 1262.

Smolenskiĭ, G.A., Bokiv, V.A., Isupov, V.A., Kraĭnik, N.N., Pasynkov, R.E., Sokolov, A.I. and Yushin, N.K. (1985) Physics of Ferroelectric Phenomena. Nauka, Leningrad.

Velbel, M.A., Long, D.T. and Gooding, J.L. (1991) Terrestrial weathering of Antarctic stone meteorites: Formation of Mg-carbonates on ordinary chondrites. Geochimica et Cosmochimica Acta, 55, 67-76.

Wang, X.B., Shen, Z.X., Hu Z.P., Qin L., Tang, S.H. and Kouk, M.H. (1996) Modulated phases in $NaNbO_3$: Raman scattering, synchrotron x-ray

diffraction, and dielectric investigations, Journal of Molecular Structure, 385, 1.

Xu, J.-A., Mao, H.-K. and Bell, P.M. (1986) High-pressure ruby and diamond fluorescence: Observations at 0.21 to 0.55 terapascal. Science, 232, 1404-1406.

Yuzyuk, Y.I., Simon, P., Gagarina, E., Hennet, L., Thiaudière, D., Torgashev, V.I., Raevskaya, S.I., Raevskii, I.P., Reznitchenko, L.A. and Sauvajol, J.L. (2005) Modulated phases in $NaNbO_3$: Raman scattering, synchrotron x-ray diffraction, and dielectric investigations. Journal of Physics: Condensed Matter, 17, 4977-4990.

Zhelnova, O.A., Smotrakov, V.G., Paevskii, I.P. and Fesenko, E.G. (1983) Region of bladed crystallization of $NaNbO_3$ in the Na_2O-Nb_2O_5-B_2O_3 system. Soviet Physics, Crystallography, 28, 5, 623-624.

VITA

Cara K. Mulcahy was born in Lancaster, CA on June 11, 1979. She was raised in Roanoke, VA where she graduated from Northside High School in May 1997. She attended Virginia Western Community College where she graduated with her Associate's in Science Degree in 1999. Her Bachelor's degree was completed at the University of Virginia, Charlottesville in May 2001. She attended core courses in geosciences at Virginia Polytechnic Institute and State University in Blacksburg, VA before beginning her Master's in Earth and Planetary Sciences at the University of Tennessee, Knoxville.